Pathways of peroxynitrite oxidation of thiol groups

Celia QUIJANO*, Beatriz ALVAREZ*, Reynaldo M. GATTI†, Ohara AUGUSTO† and Rafael RADI*‡

*Departamento de Bioquímica, Facultad de Medicina, Universidad de la República, Av. Gral. Flores 2125, 11800 Montevideo, Uruguay, and †Departamento de Bioquímica, Instituto de Química, Universidade de São Paulo, C.P. 26.077-970, São Paulo, Brasil

Peroxynitrite mediates the oxidation of the thiol group of both cysteine and glutathione. This process is associated with oxygen consumption. At acidic pH and a cysteine/peroxynitrite molar ratio of $\leqslant 1.2$, there was a single fast phase of oxygen consumption, which increased with increasing concentrations of both cysteine and oxygen. At higher molar ratios the profile of oxygen consumption became biphasic, with a fast phase (phase I) that decreased with increasing cysteine concentration, followed by a slow phase (phase II) whose rate of oxygen consumption increased with increasing cysteine concentration. Oxygen consumption in phase I was inhibited by desferrioxamine and 5,5-dimethyl-1-pyrroline *N*-oxide, but not by mannitol; superoxide dismutase also inhibited oxygen consumption in phase I, while catalase added during phase II decreased the rate of oxygen consumption. For both cysteine and glutathione, oxygen consumption in phase I was maximal at neutral to acidic pH; in contrast, total thiol oxidation was maximal at alkaline pH. EPR spin-trapping studies using *N-tert*-butyl-α-phenylnitrone indicated that the yield of thiyl radical adducts had a pH profile comparable with that found for oxygen consumption. The apparent second-order rate constants for the reactions of peroxynitrite with cysteine and glutathione were 1290 ± 30 $M^{-1} \cdot s^{-1}$ and 281 ± 6 $M^{-1} \cdot s^{-1}$ respectively at pH 5.75 and 37 °C. These results are consistent with two different pathways participating in the reaction of peroxynitrite with low-molecular-mass thiols: (a) the reaction of the peroxynitrite anion with the protonated thiol group, in a second-order process likely to involve a two-electron oxidation, and (b) the reaction of peroxynitrous acid, or a secondary species derived from it, with the thiolate in a one-electron transfer process that yields thiyl radicals capable of initiating an oxygen-dependent radical chain reaction.

INTRODUCTION

Peroxynitrite anion ($ONOO^-$), the product of the reaction between superoxide anion ($O_2^{\bullet -}$) and nitric oxide ($^{\bullet}NO$), and its conjugated acid, peroxynitrous acid (ONOOH) ($pK_A = 6.8$ at 37 °C [1,2]) are potent oxidants known to be formed *in vivo* [3–5] and to oxidize a wide range of biological targets, including thiol groups [1,6–8]. [Note that the IUPAC recommended names for peroxynitrite anion ($ONOO^-$), peroxynitrous acid (ONOOH) and nitric oxide ($^{\bullet}NO$) are oxoperoxonitrate(1−), hydrogen oxoperoxonitrate and nitrogen monoxide respectively.]

Peroxynitrite anion is a relatively stable species; however, peroxynitrous acid decays, rearranging to nitrate with a half-life of less than 1 s at physiological pH and 37 °C [2]. On the basis of kinetic studies, two pathways have been proposed for the peroxynitrite-mediated oxidation of substrates. In the first mechanism, peroxynitrite reacts with target molecules in an overall second-order process. (The term peroxynitrite is used to refer to the sum of both $ONOO^-$ and its conjugated acid, ONOOH. When a specific species is referred to, it is named peroxynitrite anion or peroxynitrous acid respectively.) In the second mechanism, peroxynitrous acid, in the pathway to nitrate, is converted in a rate-limiting step into a species with a reactivity similar to that of the hydroxyl radical, which can attack targets due to its strong oxidizing properties ($E_0' = +2.1$ V [2]), resulting in a zero-order process with respect to substrate. This species is presumed to be a vibrationally activated intermediate of peroxynitrous acid [2], and has been referred to as ONOOH* [9] (eqn. 1), although controversy exists as whether the oxidant may be hydroxyl ($^{\bullet}OH$) or nitrogen dioxide ($^{\bullet}NO_2$) radicals, formed from the homolytic cleavage of peroxynitrous acid, or even a *trans* conformer of peroxynitrous acid [10,11] (for a critical discussion, see [9,11]).

$$ONOO^- + H^+ \rightleftharpoons ONOOH \xrightarrow{k_H'} [ONOOH^*] \rightarrow NO_3^- + H^+ \qquad (1)$$

The first description of second-order kinetics during the reaction of peroxynitrite and a target molecule was for reactions with thiol groups [1]. The second-order rate constants for the reactions of peroxynitrite with cysteine, glutathione and the single thiol group of albumin at pH 7.4 and 37 °C are 4500 $M^{-1} \cdot s^{-1}$ [1], 1350 $M^{-1} \cdot s^{-1}$ [2] and 2700 $M^{-1} \cdot s^{-1}$ [1] respectively.

In the reaction of peroxynitrite with the thiol groups of cysteine and albumin, maximum oxidation yields were found at alkaline pH [1]; desferrioxamine, a scavenger of peroxynitrous acid [10], failed to inhibit this oxidation at pH 7.3 and 8.0. This led to the suggestion that peroxynitrite anion, rather than peroxynitrous acid, was the main reactive species towards thiols [1]. However, a significant fraction of cysteine was still oxidized at acidic pH, where most peroxynitrite would be protonated and could be converted into secondary oxidizing species.

Peroxynitrite oxidation of thiols occurs, at least partially, through one-electron-transfer oxidation processes, since EPR spin-trapping studies of the peroxynitrite-mediated oxidation of cysteine, glutathione and the thiol group of albumin demonstrated that the corresponding thiyl radicals were formed [12–14]. Alternatively, peroxynitrite could oxidize thiols via a two-electron oxidation process, without the formation of free-radical

Abbreviations used: DTNB, 5,5′-dithiobis-(2-nitrobenzoic acid); DMPO, 5,5-dimethyl-1-pyrroline *N*-oxide; PBN, *N-tert*-butyl-α-phenylnitrone; DTPA, diethylenetriaminepenta-acetic acid.

‡ To whom correspondence should be addressed.

intermediates. However, product formation would not discriminate between one- and two-electron routes, as the main product of both processes is the corresponding disulphide (i.e. cystine and glutathione disulphide).

It is likely that peroxynitrite-mediated thiol oxidation will, in fact, occur through competing one- and two-electron pathways, as seen for methionine [15]. In order to better establish the pathways involved, we examined the reaction of the oxidant, in aerobic media, with both cysteine and glutathione by kinetic analysis and by measurement of total thiol oxidation yields, oxygen consumption and thiyl radical formation. We also assessed the role of the one-electron oxidation of thiols by peroxynitrite in triggering secondary, oxygen-dependent, free-radical chain reactions.

EXPERIMENTAL

Materials

Cysteine, glutathione, hydrogen peroxide, potassium phosphate (mono- and di-basic), 5,5′-dithiobis-(2-nitrobenzoic acid) (DTNB), desferrioxamine, ethanol, formate, mannitol, DMSO, 5,5-dimethyl-1-pyrroline *N*-oxide (DMPO), *N*-*tert*-butyl-α-phenylnitrone (PBN), diethylenetriaminepenta-acetic acid (DTPA), sulphanilamide, *N*-(1-naphthyl)ethylenediamine, Sephadex G-25, catalase and Chelex-100 were obtained from Sigma Chemical Co. (St. Louis, MO, U.S.A.). Superoxide dismutase (2100 units/mg) was a gift from Grunenthal (Aachen, Germany). Oxygen, nitrogen and argon gas were obtained from Aga Gas Co. (Montevideo, Uruguay).

DMPO was purified by vacuum distillation and PBN was recrystallized from hexane [16]. Cysteine and glutathione solutions were prepared daily prior to use, in deoxygenated, highly pure water (Barnstead ultra pure water system), and kept in the dark at 4 °C under argon or nitrogen.

Peroxynitrite was synthesized in a quenched-flow reactor as previously described [1], and excess hydrogen peroxide was removed by treatment with MnO_2. Peroxynitrite concentrations were determined spectrophotometrically at 302 nm ($\epsilon = 1670\ M^{-1}\cdot cm^{-1}$).

Superoxide dismutase inactivation

Superoxide dismutase (17 μM) was partially inactivated by incubation with 18 mM hydrogen peroxide in 50 mM potassium pyrophosphate, pH 10, for 1 h at 25 °C [17]. Excess hydrogen peroxide was eliminated by size-exclusion chromatography using a Sephadex G-25 column; 70 % inactivation of superoxide dismutase was achieved. Higher concentrations of hydrogen peroxide to increase inactivation yields were avoided because they can cause copper release from the active site [18]. Protein concentrations were assessed using the Bradford assay [19], and enzymic activity was determined by measuring the inhibition of the xanthine oxidase-mediated reduction of cytochrome c^{3+} monitored at 550 nm [20].

Oxygen consumption studies

Oxygen consumption was measured polarographically using a Cole Parmer oximeter fitted with a water-jacketed Clark-type electrode (YSI Model 5300), calibrated with air-saturated distilled water (oxygen concentration 170–195 μM at 37 °C). All the experiments were carried out at 37 °C in 100 mM potassium phosphate buffer and 0.1 mM DTPA.

Different oxygen concentrations were achieved by bubbling the buffer solution placed in the 1 ml chamber of the oxygen electrode with either nitrogen or oxygen for various periods of time (0.1–1 min). Oxygen concentrations reported correspond to those measured by the electrode immediately before the addition of peroxynitrite.

Thiol quantification

Thiol groups were measured using Ellman's method with DTNB at 412 nm ($\epsilon_{412} = 1.36 \times 10^4\ M^{-1}\cdot cm^{-1}$ [21]), as described previously [1].

Nitrite quantification

Nitrite production during the reaction of peroxynitrite with cysteine was determined by the Griess assay [22] using sodium nitrite as a standard. The experiments were carried out at 37 °C in 100 mM potassium phosphate buffer and 0.1 mM DTPA.

Kinetic experiments

Peroxynitrite decomposition in the presence of cysteine and glutathione was studied by stopped-flow absorbance spectroscopy at 302 nm using an Applied Photophysics SF.17MV spectrophotometer (Leatherhead, U.K.) with a mixing time of less than 2 ms. Reactions were initiated at 36.8 °C by mixing equal volumes of solutions A and B. Solution A consisted of 100 mM phosphate buffer, pH 5.5, containing 0.1 mM DTPA and the thiol. Solution B was peroxynitrite diluted immediately before use to 0.4 mM with distilled water containing 0.1 mM DTPA. The final pH of the mixtures, measured at the outlet, was 5.75 ± 0.03. The kinetics of peroxynitrite decomposition were fitted to a pseudo-first-order reaction equation by non-linear regression.

EPR experiments

EPR spectra were recorded at room temperature using a Bruker ER 200 D-SRC spectrometer. The incubation mixtures (final volume 500 μl) at room temperature were transferred to flat cells immediately after peroxynitrite addition, and spectra were recorded after a 1 min incubation. The phosphate buffer used in EPR experiments was treated with Chelex-100 to remove iron contamination.

Data analysis

Experiments reported herein were performed a minimum of three times, with similar results being obtained. Results are expressed as means $\pm$ S.D. Graphics and curve fitting were generated in Slide-Write 2.1 for Windows (Advanced Graphics Software Inc.).

RESULTS

Oxygen consumption

The peroxynitrite-mediated oxidation of both cysteine and glutathione was associated with oxygen consumption (Figure 1), in agreement with a recent report [23]. At a cysteine/peroxynitrite molar ratio of $\geqslant 1.2$, there was a single (fast) phase of oxygen consumption that lasted less than 0.5 min (Figure 1a), in which the total consumption increased as the concentration of cysteine increased (Figure 2). When the cysteine/peroxynitrite molar ratio was $\leqslant 1.2$, oxygen consumption acquired a new profile, consisting of two phases (Figure 1b): a fast phase (phase I), in which oxygen consumption decreased with cysteine concen-

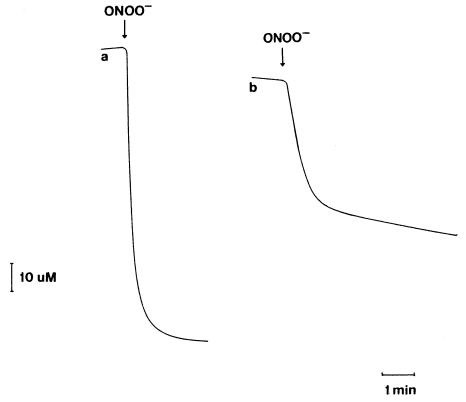

Figure 1 Oxygen consumption profiles

(**a**) Peroxynitrite (0.70 mM) was added to cysteine (0.8 mM); oxygen consumption occurred in a single fast phase (phase I). (**b**) Peroxynitrite (0.70 mM) was added to cysteine (4 mM), and oxygen consumption occurred in two phases: a fast phase (phase I) followed by a slow one (phase II). Both experiments were carried out in potassium phosphate buffer, pH 5.8.

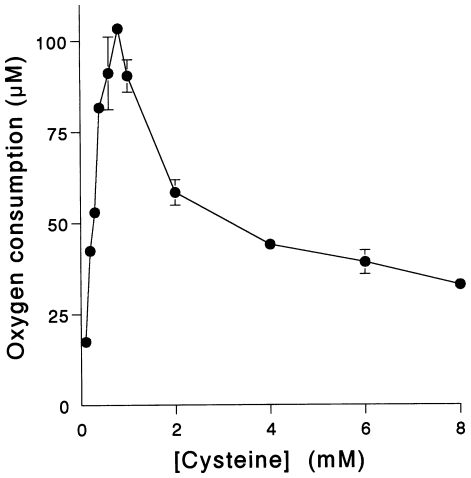

Figure 2 Oxygen consumption (phase I) as a function of cysteine concentration

Reactions were initiated by the addition of peroxynitrite (0.70 mM) to various concentrations of cysteine (0.1–10 mM). Experimental conditions were as in Figure 1. Values are means ± S.D., $n = 3$.

Table 1 Effect of cysteine concentration on oxygen consumption

Peroxynitrite (0.7 mM) was added to different concentrations of cysteine and incubated at 37 °C in 100 mM potassium phosphate, pH 5.8. Oxygen consumption in phase I occurred within less than 0.5 min; rates of oxygen consumption in phase II were measured in the first 5 min period, during which they remained constant.

	Oxygen consumption	
Cysteine (mM)	Phase I (μM)	Phase II (μM/min)
1	87 ± 2	0.27 ± 0.04
2	59 ± 3	0.95 ± 0.08
4	44 ± 1	2.77 ± 0.20
6	39 ± 3	3.69 ± 0.27
10	32 ± 2	5.48 ± 0.87

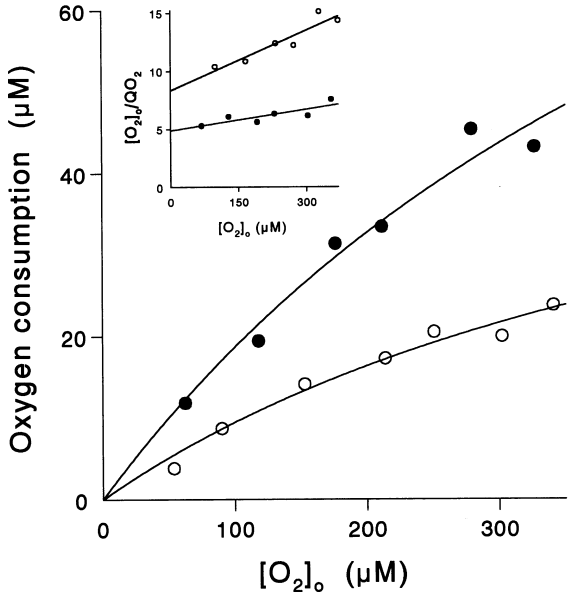

Figure 3 Oxygen consumption (phase I) as a function of oxygen concentration

Cysteine (1 mM) was incubated in potassium phosphate buffer, pH 5.6, and 0.70 mM (●) or 0.35 mM (○) peroxynitrite was added. The oxygen concentration ($[O_2]_o$) was varied as described in the Experimental section. The inset shows a secondary Hanes plot of the results; QO_2 is oxygen consumption.

tration (Figure 2), followed by a slow phase (phase II), in which the rate of oxygen consumption increased with cysteine concentration (Table 1).

The slow phase of oxygen consumption was remarkably long, lasting for several hours. For instance, in a system consisting of cysteine (4 mM) and peroxynitrite (0.7 mM) in 100 mM potassium phosphate buffer, pH 5.5, and 37 °C, the slow phase lasted for and slowly decreased over a 210 min observation period, at the end of which the rate of oxygen consumption was 3% of the initial rate. During this experiment, several reoxygenations were carried out so as to maintain the oxygen concentration above 50% of the initial concentration.

Oxygen consumption as a function of oxygen concentration was assessed at two different concentrations of peroxynitrite (0.70 and 0.35 mM), with cysteine (5 mM) in excess. The total oxygen consumption in phase I increased as a hyperbolic function of oxygen concentration (Figure 3); secondary Hanes plots yielded maximum oxygen consumptions of 164 ± 33 and 58 ± 8 μM respectively at pH 5.6 and 37 °C (Figure 3, inset), which are equivalent to 0.23 and 0.17 mol of oxygen consumed/mol of peroxynitrite respectively.

Oxygen consumption in phase I was maximal at neutral to acidic pH (Figure 4), displaying a pH-dependent profile in contrast with that obtained for the total thiol oxidation yields (Figure 4, inset). Values of 0.19 and 0.07 mol of oxygen consumed/mol of peroxynitrite were measured at pH 7 and 9 respectively. Maximum oxygen consumption obtained for the peroxynitrite-mediated oxidation of glutathione also occurred at neutral pH, but a bell-shaped profile was obtained, with oxygen consumption decreasing in both the acidic and alkaline ranges (Figure 4). In this case, values of 0.15 and 0.05 mol of oxygen

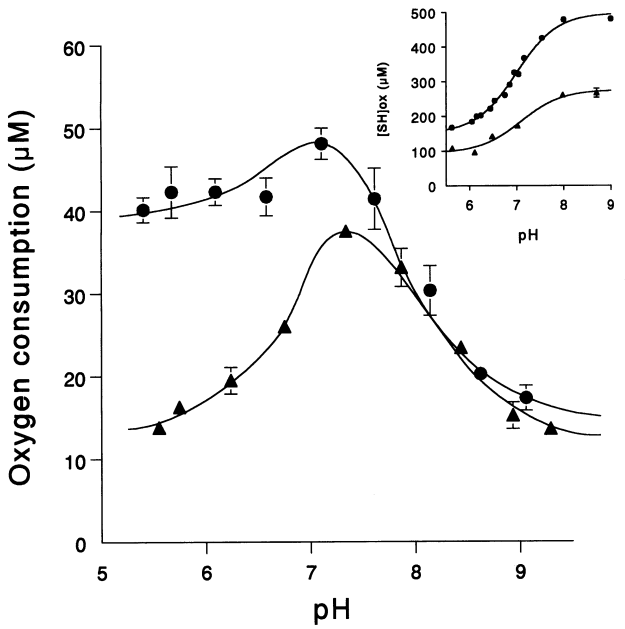

Figure 4 Oxygen consumption as a function of pH

Reactions were started by the addition of 0.25 mM peroxynitrite to 0.5 mM glutathione (▲) or cysteine (●). The inset shows the thiol oxidation, assessed by Ellman's method, of the reaction of 0.5 mM glutathione or cysteine with peroxynitrite under the same conditions; [SH]ox, oxidized thiol groups. Data are means ± S.D., $n = 3$.

Table 2 Effects of scavengers on oxygen consumption

Cysteine (1 mM) was incubated in the presence of the scavenger in 100 mM potassium phosphate, pH 5.7, at 37 °C, and peroxynitrite (0.7 mM) was added to the reaction mixture. Oxygen consumption, measured in phase I, was 67 ± 7 μM in the absence of scavengers.

Compound	Concentration	Inhibition (%)
Desferrioxamine	50 μM	8 ± 1
	150 μM	20 ± 3
DMPO	25 mM	82 ± 4
	50 mM	88 ± 5
Mannitol	130 mM	0
	260 mM	0

consumed/mol of peroxynitrite were obtained at neutral and alkaline pH respectively. However, the maximum oxidation yields for cysteine and glutathione were obtained at alkaline pH (Figure 4, inset). Nitrite production increased with increasing concentrations of cysteine, and was higher at alkaline pH. For instance, during peroxynitrite (500 μM) reaction with cysteine (125 μM), nitrite formation was 41 ± 19 and 84 ± 17 μM at pH 5.7 and 8.2 respectively.

Effects of scavengers, superoxide dismutase and catalase on oxygen consumption

Different scavengers known to interact either with peroxynitrous acid or with hydroxyl radicals were assessed for their ability to inhibit oxygen consumption. Co-incubation of desferrioxamine, postulated to react with *trans*-peroxynitrous acid [10], and

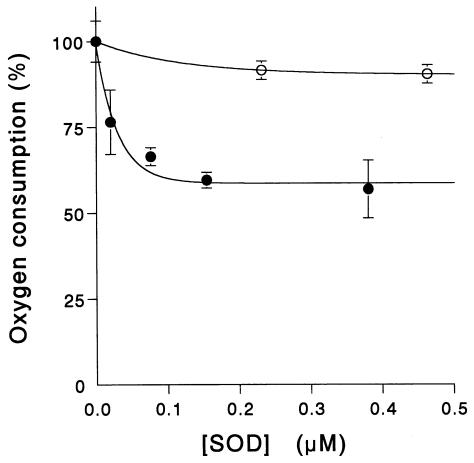

Figure 5 Effect of superoxide dismutase on oxygen consumption

Peroxynitrite (0.70 mM) was added to 1 mM cysteine in potassium phosphate buffer, pH 5.9, in the presence of different concentrations of active (●) or 70%-inactivated (○) superoxide dismutase (SOD). Data are means ± S.D., $n = 3$.

DMPO with cysteine (1 mM) at pH 5.7 resulted in a dose-dependent inhibition of oxygen consumption (Table 2). Mannitol, a well known hydroxyl radical scavenger, did not inhibit oxygen consumption up to a concentration of 260 mM (Table 2). The actions of other hydroxyl radical scavengers, such as DMSO, ethanol and formate, could not be evaluated because their reaction with peroxynitrite results itself in oxygen consumption.

In the presence of superoxide dismutase, oxygen consumption in phase I decreased to 57 ± 2 % of the original value (Figure 5). Reactions using similar concentrations of partially inactivated (70 %) superoxide dismutase showed a small decrease in oxygen uptake (91 ± 3 % of control), which was probably due to the remaining superoxide dismutase activity. Catalase (490 units · ml^{-1}) added at different times during phase II under conditions similar to those for Figure 1(b) (but with 6 mM cysteine) resulted in oxygen evolution (4.9 μM at 2.5 min; 5.4 μM at 11 min); the rate of oxygen consumption was decreased to 80 % of the initial value (results not shown).

EPR experiments

The formation of thiyl radicals during the peroxynitrite-mediated oxidation of glutathione has been demonstrated previously by spin-trapping experiments in the presence of DMPO. In that case, however, a composite EPR spectrum consisting of two radical adducts, the DMPO-hydroxyl and the DMPO-glutathionyl adducts, was obtained. Since the EPR spectra of these adducts overlap, it is difficult to estimate the yield of thiyl radicals formed [12]. Consequently, we performed spin-trapping experiments with another spin-trap, PBN, which does not give stable hydroxyl radical adducts. As shown in Figure 6, incubation of cysteine or glutathione with peroxynitrite in the presence of PBN led to the detection of the characteristic PBN-cysteinyl ($a_N = 1.55$ mT; $a_H = 0.35$ mT) [24] (Figure 6A) and PBN-glutathionyl ($a_N = 1.55$ mT; $a_H = 0.31$ mT) (Figure 6B) adducts. To the best of our knowledge, the latter radical adduct has not been reported before, but its EPR parameters are as expected for PBN-thiyl radical adducts [24].

The yield of PBN-thiyl radical adducts obtained in incubations of peroxynitrite with cysteine and glutathione as a function of pH presented profiles very similar to those obtained for maximum

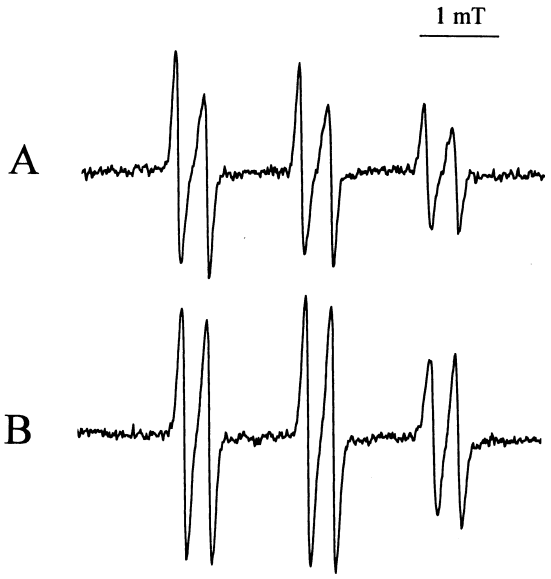

Figure 6 EPR spectra of PBN-radical adducts obtained during peroxynitrite decomposition in the presence of cysteine and glutathione

The spectra were obtained 1 min after the addition of 0.8 mM peroxynitrite to incubation mixtures in 0.3 M potassium phosphate buffer, pH 6.0, containing 50 mM PBN, 0.1 mM DTPA and (**A**) 10 mM cysteine or (**B**) 10 mM glutathione. Instrument conditions: microwave power, 20 mW; modulation amplitude, 0.1 mT; time constant, 0.2 s; scan rate, 0.05 mT/s; gain, 5×10^5.

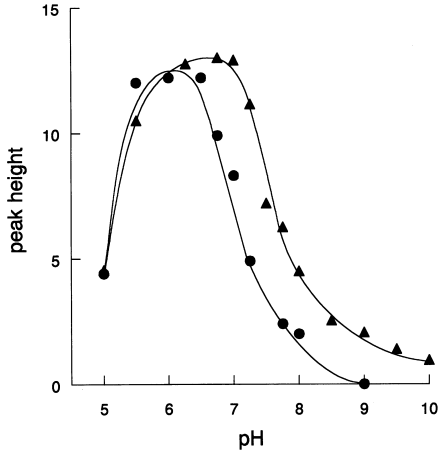

Figure 7 Effect of pH on the yields of PBN-thiyl radical adducts obtained during the peroxynitrite-mediated oxidation of cysteine and glutathione

The spectra were obtained 1 min after the addition of 0.80 mM peroxynitrite to incubation mixtures containing 50 mM PBN, 0.1 mM DTPA and 10 mM cysteine (●) or glutathione (▲) in 0.3 M potassium phosphate buffer, the pH of which was varied. The instrument conditions were the same as in Figure 6, except that the gain was changed depending on the radical adduct yield. The measured peak height corresponds to the low-field peak of the corresponding PBN-thiyl radical adduct.

oxygen consumption (Figure 7), indicating that oxygen consumption is triggered by the formation of thiyl radicals.

Kinetics of peroxynitrite decomposition

The disappearance of peroxynitrite (0.2 mM) at pH 5.75 and 37 °C in the presence of a 5–100-fold excess of cysteine or

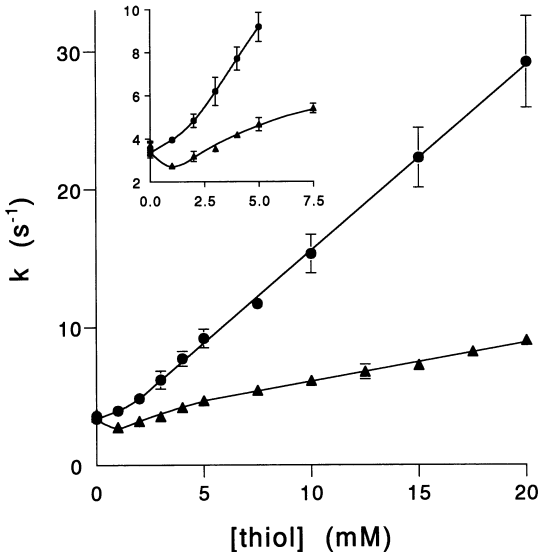

Figure 8 Peroxynitrite decomposition rates in the presence of cysteine and glutathione

Peroxynitrite (0.2 mM) was mixed with various amounts of cysteine (●) or glutathione (▲) in 50 mM potassium phosphate, 0.1 mM DTPA, pH 5.75 ± 0.01, at 36.8 °C. The kinetics of peroxynitrite decomposition were fitted to a single exponential function by non-linear regression. The inset shows peroxynitrite decomposition rate as a function of thiol concentration in the concentration range 0–7.5 mM. Data are means ± S.D. of at least seven different runs.

glutathione was assessed. Under these experimental conditions the proton-catalysed decomposition of peroxynitrite occurs, with $k_H' = 3.49 \pm 0.11\ s^{-1}$ (Figure 8). Plots of the apparent rate constant against the cysteine concentration were linear, except for a small but reproducible upward curvature at low concentrations. The apparent second-order rate constant for the reaction with cysteine at this pH was $k_S' = 1290 \pm 30\ M^{-1} \cdot s^{-1}$, consistent with our previous work [1] (Figure 8).

In the reaction with glutathione, peroxynitrite decomposition followed pseudo-first-order kinetics, with an apparent second-order rate constant of $281 \pm 6\ M^{-1} \cdot s^{-1}$, in the presence of glutathione concentrations of $\geqslant 5$ mM. At lower concentrations a peculiar profile was observed: with glutathione at $\leqslant 2$ mM, a decrease in the apparent decomposition rate with respect to the proton-catalysed decomposition was observed, and between 2 and 5 mM glutathione the decomposition constants increased with the concentration of glutathione, presenting a downward curve (Figure 8).

DISCUSSION

Two reaction pathways appear to be operative for the oxidation of cysteine and glutathione by peroxynitrite. One pathway predominates at alkaline pH, presenting low oxygen consumption and thiyl radical yields but with the highest yields of thiol oxidation and nitrite formation. Another pathway prevails at neutral to acidic pH which is characterized by high oxygen consumption and thiyl radical formation, but is associated with low yields of thiol oxidation. These observations suggest that the first pathway is related to the second-order reaction of the protonated thiol group with peroxynitrite anion [1]; the latter will oxidize the thiol without the formation of thiyl radicals, and thus with no associated oxygen consumption. In this pathway, the peroxynitrite anion would participate as a two-electron oxidant [9], leading to the formation of nitrite and the unstable

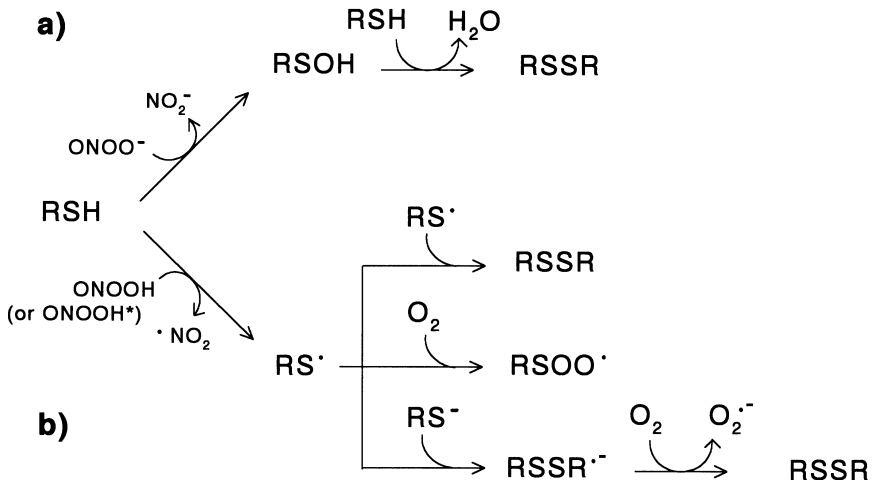

Scheme 1 Peroxynitrite oxidation pathways

(**a**) Two-electron oxidation pathway. Peroxynitrite reacts with the thiol group producing the unstable sulphenic acid, which in turn reacts with another thiol yielding the disulphide. (**b**) One-electron oxidation pathway. Peroxynitrous acid, or a secondary species derived from it, reacts with the thiol producing the thiyl radical. The latter can dimerize to the disulphide, or can react with oxygen to produce the peroxyl radical or with the thiolate yielding the disulphide radical anion.

sulphenic acid, which will rapidly react with another thiol yielding the corresponding disulphide. In the second pathway, more relevant at acidic pH, peroxynitrous acid, or a secondary oxidizing species derived from it, participates in thiol oxidation in a one-electron transfer mechanism, giving rise to nitrogen dioxide and thiyl radical; the latter is able to participate in reactions responsible for oxygen consumption or to combine with another thiyl radical to form disulphides. Evidently, the two pathways coexist and compete at a given pH (Scheme 1).

The bell-shaped profile of oxygen consumption as a function of cysteine concentration observed in Figure 2 suggests that the one-electron oxidizing species at acidic pH is a secondary intermediate derived from peroxynitrous acid in a process that is zero-order with respect to thiol. Thus, at low cysteine/peroxynitrite molar ratios, the formation of this intermediate predominates, leading to the formation of thiyl radicals and resulting in oxygen consumption. At higher cysteine/peroxynitrite ratios, oxygen consumption decreases as the second-order reaction of peroxynitrite with cysteine becomes more significant.

According to the proposed pathways, the rate of peroxynitrite decomposition in the presence of thiols could be written as:

$$\frac{-\mathrm{d}[\mathrm{ONOO^-}]}{\mathrm{d}t} = k_{\mathrm{H}}'[\mathrm{ONOO^-}] + k_{\mathrm{S}}'[\mathrm{SH}][\mathrm{ONOO^-}] \quad (2)$$

where k_{H}' and k_{S}' are the kinetic constants for the two pathways of peroxynitrite reactivity with thiols. These can be described by eqns. (3) and (4) [1,25] respectively:

$$k_{\mathrm{H}}' = \frac{k_{\mathrm{H}}[\mathrm{H^+}]}{K_{\mathrm{A1}} + [\mathrm{H^+}]} \quad (3)$$

$$k_{\mathrm{S}}' = \frac{k_{\mathrm{S}} K_{\mathrm{A1}}[\mathrm{H^+}]}{(K_{\mathrm{A1}} + [\mathrm{H^+}])(K_{\mathrm{A2}} + [\mathrm{H^+}])} \quad (4)$$

where k_{S} is the second-order rate constant of the reaction of cysteine with the peroxynitrite anion, k_{H} is the first-order rate constant for peroxynitrite decomposition (4.5 s^{-1} at 37 °C [2]), and K_{A1} and K_{A2} are the dissociation constants for peroxynitrite ($pK_{\mathrm{A1}} = 6.8$) and cysteine ($pK_{\mathrm{A2}} = 8.3$) respectively. Thus, according to eqn. (2), at pH $\leqslant 7$ and 0.5 mM cysteine, the pathway zero-order with respect to the thiol concentration accounts for 50 % or more of the total reactivity of peroxynitrite.

The inhibition studies (Table 2) in the presence of desferrioxamine and mannitol support the view that peroxynitrous acid or, most likely, a secondary species derived from it (i.e. *trans*-peroxynitrous acid or the vibrationally activated intermediate ONOOH* [9–11]), and not the hydroxyl radical, is the one-electron oxidant. The high percentage inhibition obtained with DMPO relies on its reaction with both peroxynitrite and the thiyl radical [12].

The fact that a steeper decrease in oxygen consumption and thiyl radical yield was observed at acidic pH for glutathione than for cysteine (Figures 4 and 7) is in agreement with a preferential reaction of the one-electron oxidizing species with the corresponding thiolate. Indeed, since the pK_{A} of glutathione is significantly higher than that of cysteine (values of 9.4 and 8.3 respectively at 37 °C [26]), the dissociated form of glutathione will be present at much lower concentrations at acidic pH.

The slow phase of oxygen consumption observed at cysteine/peroxynitrite molar ratios of $\geqslant 1.2$ (Figure 1) indicates that radical chain reactions were taking place. In aerobic media, thiyl radicals can yield a number of secondary radicals, including the peroxyl radical ($RSOO^{\bullet}$) and the disulphide radical anion ($RSSR^{\bullet -}$); the latter can promote the formation of superoxide and hydrogen peroxide (see Scheme 1), as supported by the experiments with superoxide dismutase (Figure 5) and catalase. In turn, superoxide is capable of oxidizing the thiol group of glutathione, giving rise to thiyl radicals [23,27–29] or to sulphinyl radicals ($RSO^{\bullet}$) [30]:

$$O_2^{\bullet -} + \mathrm{RSH} + \mathrm{H^+} \rightarrow \mathrm{RS^{\bullet}} + H_2O_2 \quad (5)$$

$$O_2^{\bullet -} + \mathrm{RSH} \rightarrow (\mathrm{RS}\ldots O_2\mathrm{H})^{\bullet -} \rightarrow \mathrm{RSO^{\bullet}} + \mathrm{OH^-} \quad (6)$$

An increase in the cysteine concentration would favour the

formation of the disulphide radical anion from the thiyl radical, rather than reaction of the thiyl radical with molecular oxygen or its dimerization. This would contribute to the decrease in phase I oxygen consumption (Figure 2) and the increase in phase II oxygen consumption (Table 1) with increasing cysteine concentration.

Plots of oxygen consumption (phase I) as a function of oxygen concentration presented hyperbolic profiles. Considering that thiyl radicals and disulphide radical anions are the main species responsible for oxygen consumption, a 1:1 stoichiometry (mol of oxygen consumed/mol of thiyl radicals formed) can be assumed. Thus molar ratios of maximum oxygen consumption/peroxynitrite of approx. 0.20 would represent an upper estimate of the fraction of peroxynitrite that reacts with thiols in a one-electron oxidation process. These values agree with those previously obtained for the oxidation yields of substrates that react with peroxynitrite with zero-order kinetics [6,11,31]. We consider this to be an upper estimate because other species, such as superoxide, peroxyl radicals or sulphinyl radicals, might also be involved in the generation of thiyl radicals.

Both cysteine and glutathione presented second-order kinetics at high thiol concentrations. However, deviations from linearity were observed at low concentrations. The downward curve observed for glutathione could be considered as kinetic evidence for the formation of the activated intermediate of peroxynitrous acid, as described in the reaction of peroxynitrite with methionine [15] and tryptophan [32]. The reasons for the decrease in the decomposition rate for glutathione and the upward curvature observed for cysteine are still uncertain, but they may rely on the formation of hydrogen-bonded complexes between peroxynitrite and the thiol group, as has been observed for hydrogen peroxide [31].

Although under physiological intracellular conditions (pH 7.4, 37 °C, 5–10 mM glutathione) the second-order reaction (i.e. two-electron oxidation) of peroxynitrite with thiols would prevail quantitatively ($> 90\%$ [33]) over the one-electron oxidation process, the formation of thiyl radicals initiates an oxygen-dependent radical chain reaction that could greatly amplify the importance of the one-electron oxidation pathway in promoting peroxynitrite-dependent cellular oxidative stress.

We thank Daniel Anselmi for help in the presentation of the artwork, and our colleagues for helpful discussions. This work was supported by grants from CONICYT (Uruguay) and SAREC (Sweden) to R.R., and from FAPESP, CNPq and FINEP (Brazil) to O.A.; B.A. was partially supported by a fellowship from PEDECIBA and CONICYT (Uruguay).

Received 4 June 1996/24 September 1996; accepted 1 October 1996

REFERENCES

1 Radi, R., Beckman, J. S., Bush, K. M. and Freeman, B. A. (1991) J. Biol. Chem. **266**, 4244–4250
2 Koppenol, W. H., Pryor, W. A., Moreno, J. J., Ischiropoulos, H. and Beckman, J. S. (1992) Chem. Res. Toxicol. **5**, 834–842
3 Beckman, J. S., Ye, Y. Z., Anderson, P., Chen, J., Accavitti, M. A., Tarpey, M. M. and White, C. R. (1994) Biol. Chem. Hoppe-Seyler **375**, 81–88
4 Beckman, J. S., Chen, J., Crow, J. P. and Ye, Y. Z. (1994) Prog. Brain Res. **103**, 371–380
5 Royall, J. A., Kooy, N. W. and Beckman, J. S. (1995) New Horiz. **3**, 113–122
6 Beckman, J. S., Beckman, T. W., Chen, J., Marshall, P. A. and Freeman, B. A. (1990) Proc. Natl. Acad. Sci. U.S.A. **87**, 1620–1624
7 Radi, R., Beckman, J. S., Bush, K. M. and Freeman, B. A. (1991) Arch. Biochem. Biophys. **288**, 481–487
8 Moreno, J. J. and Pryor, W. A. (1992) Chem. Res. Toxicol. **5**, 425–431
9 Pryor, W. A. and Squadrito, G. L. (1995) Am. J. Physiol. **268**, L699–L722
10 Denicola, A., Souza, J., Gatti, R. M., Augusto, O. and Radi, R. (1995) Free Radical Biol. Med. **19**, 11–19
11 Crow, J. P., Spruell, C., Chen, J., Gunn, C., Ischiropoulos, H., Tsai, M., Smith, C. D., Radi, R., Koppenol, W. H. and Beckman, J. S. (1994) Free Radical Biol. Med. **16**, 331–338
12 Augusto, O., Gatti, R. M. and Radi, R. (1994) Arch. Biochem. Biophys. **310**, 118–125
13 Vasquez-Vivar, J., Santos, A. M., Junqueira, U. B. C. and Augusto, O. (1996) Biochem. J. **314**, 869–876
14 Gatti, R. M., Radi, R. and Augusto, O. (1994) FEBS Lett. **348**, 287–290
15 Pryor, W. A., Jin, X. and Squadrito, G. L. (1994) Proc. Natl. Acad. Sci. U.S.A. **91**, 11173–11177
16 Augusto, O. (1989) in Handbook of Biomedicine of Free Radicals and Antioxidants (Mogul, J., ed.), vol. 3, pp 193–208, CRC Press, Boca Raton, FL
17 Radi, R., Cosgrove, T. P., Beckman, J. S. and Freeman, B. A. (1993) Biochem. J. **290**, 51–57
18 Jewett, S. L., Cushing, S., Gillespie, F., Smith, D. and Sparks, S. (1989) Eur. J. Biochem. **180**, 569–575
19 Bradford, M. M. (1976) Anal. Biochem. **72**, 248–254
20 McCord, J. M. and Fridovich, I. (1969) J. Biol. Chem. **244**, 6049–6055
21 Ellman, G. L. (1959) Arch. Biochem. Biophys. **80**, 70–77
22 Green, L., Wagner D., Glogowski, J., Skipper P., Wishnok, J. and Tannerbaum, R. (1982) Anal. Biochem. **126**, 131
23 Karoui, H., Hogg, N., Fréjaville, C., Tordo, P. and Kalyanaraman, B. (1996) J. Biol. Chem. **271**, 6000–6009
24 Buettner, G. R. (1987) Free Radical Biol. Med. **3**, 259–302
25 Keith, W. G. and Powell, R. E. (1969) J. Chem. Soc. A, 90
26 Torchinsky, Y. M. (1981) in Sulfur in Proteins, pp. 3–8, Pergamon Press, New York
27 Winterbourn, C. C. (1993) Free Radical Biol. Med. **14**, 85–90
28 Prutz, W. A., Butler, J. and Land, E. J. (1994) Biophys. Chem. **49**, 101–111
29 Koppenol, W. H. (1993) Free Radical Biol. Med. **14**, 91–94
30 Winterbourn, C. C. and Metodiewa, D. (1994) Arch. Biochem. Biophys. **314**, 284–290
31 Alvarez, B., Denicola, A. and Radi, R. (1995) Chem. Res. Toxicol. **8**, 859–864
32 Alvarez, B., Rubbo, H., Kirk, M., Barnes, S., Freeman, B. A. and Radi, R. (1996) Chem. Res. Toxicol. **9**, 390–396
33 Augusto, O. and Radi, R. (1995) in Biothiols in Health and Disease (Packer, L. and Cadenas, E., eds.), pp. 83–116, Marcel Dekker, New York